Arctic-North Pacific coupled impacts on the late autumn cold in North America

Mi-Kyung Sung[1], Baek-Min Kim[1], Eun-Hyuk Baik[1],

Young-Kwon Lim[2], Seong-Joong Kim[1]

[1]Korea Polar Research Institute, Incheon, Korea

[2]NASA Goddard Space Flight Center, Global Modeling and Assimilation Office, and Goddard Earth Sciences Technology and Research, Greenbelt, USA

Keywords : Pacific Decadal Oscillation, arctic warming, midlatitude climatic impact

Abstract

The Pacific Decadal Oscillation (PDO) is known to bring an anomalously cold (warm) period to southeastern (northwestern) North America during the cold season of its positive phase through a Rossby wave linkage. This study provides evidence that the remote connection between the North Pacific and the downstream temperature over central North America is strengthened by the warm arctic conditions over the Chukchi and East Siberian Sea, especially in the late autumn season. The modulation effect of the Arctic manifests itself as an altered Rossby wave response to a transient vorticity forcing that results from an equatorward storm track shift, which is induced collaboratively by the PDO and the warm Arctic. This observational finding is supported by two independent modeling experiments: 1) an idealized coupled GCM experiment being nudged toward the warm arctic surface condition and 2) a simple stationary wave model (SWM) experiment forced by transient eddy forcing.

1. Introduction

As proximate causes for the recurrent extremely cold winters of 2009/10, 2010/11, 2013/14, and 2014/15 over North America, researchers proposed 1) changes in the wave characteristics due to the arctic sea ice loss and the arctic warming and 2) the warming in the tropical Pacific [*Stroeve et al.*, 2012; *Palmer*, 2014; *Francis and Vavrus*, 2015; *Hartmann, 2015; Kug et al.*, 2015; *Overland and Wang*, 2015;]. Compared to the arctic and the tropical impacts, the North Pacific has received less attention in association with potential impacts on the extreme weather in North America (NA). In general, the extratropical sea surface temperature (SST) anomalies are regarded as being inefficient in driving atmospheric anomalies [*Lau and Nath*, 1994; *Kushnir et al.*, 2002]. However, recent studies began to find physical role of extratropical SST [Sato et al., 2014; Simmonds and Govekar, 2014], and it is also suggested that the abnormal SST warming along the subarctic North Pacific and the western coast of NA during the 2013/14 winter played a non-negligible role in the exceptionally cold winter [*Lee et al.*, 2015].

The physical mechanism by which the extratropical SST contributes to the occurrence of extremely cold weather is not yet clear. Here, we emphasize the role of the oceanic baroclinicity and its impacts on the overlying atmosphere. Recently, analyses of observed precipitation and high-resolution modeling experiments supported the anchoring effect of the midlatitude SST on the Pacific storm track nearby the oceanic frontal zones, such as the Kuroshio-Oyashio Extension [*Sampe et*

al., 2010; *Frankignoul et al.*, 2011; *Sung et al.*, 2014]. The oceanic impacts on the high-frequency eddies have important implications for large-scale wave activity, since high-frequency eddies act to enhance low-frequency atmospheric variability [*Kug and Jin*, 2009].

This study investigates the physical links among the North Pacific SST variability, the arctic temperature, and the atmospheric circulation that brings cold weather over the NA region during the late autumn season when sea ice-related arctic warming is maximum [*Screen and Simmonds*, 2010]. Among the large-scale extratropical SST variabilities over the North Pacific, we focus on the Pacific Decadal Oscillation (PDO) in this study. It is suggested that the state of the PDO fundamentally affects the weather of North America [*Bond and Harrison*, 2000; *Sung et al.*, 2014]. Since the Aleutian low, the extratropical oceanic front, and an atmospheric wave bridge that originates from the tropics are major contributors to PDO variability [*Schneider and Cornuelle*, 2005], using the PDO index provides the benefit of reflecting both extratropical and tropical variabilities. Although the name of the PDO highlights the decadal nature of the phenomenon's variability, the interannual variability is also pronounced. This study focuses on the interannual variability of the PDO.

2. Data and model

We analyzed monthly atmospheric reanalysis data obtained from the National

Centers for Environmental Prediction/National Center for Atmospheric Research (NCEP/NCAR) [*Kalnay et al.*, 1996]. We set the analysis periods of the dataset for the years 1950 to 2011, focusing on the late autumn season (October to November). The observational PDO index was downloaded from the Joint Institute for the Study of the Atmosphere and Ocean (JISAO) website (http://jisao.washington.edu/pdo).

In order to complement the observational finding about the impact of the warm and the cold Arctic, we performed two kinds of model experiments using the Geophysical Fluid Dynamics Laboratory (GFDL) CM2.1 coupled model [*Delworth and Coauthors*, 2006] and a stationary wave model (SWM) [*Ting and Yu*, 1998]. In order to isolate the warm and cold arctic impact in the CM2.1, the SST in the high latitudes (north of 65°N) was restored to the Extended Reconstructed Sea Surface Temperature (ERSST) v3 historical reconstruction of Smith et al. [2008] covering 60 years, which began in 1951. The restoring time scale was a five-day period. Other regions are fully coupled, and five ensemble simulations were carried out with randomly chosen initial conditions (see Kug et al. [2015] for further details). The PDO index in the model output was calculated from the leading Empirical Orthogonal Function (EOF) of SST anomalies in the North Pacific basin (120E-110W, 20N-60N). Since the model is run freely except for Arctic region, the PDO evolves according to the internal dynamics of the model. It is known that the CM2.1 well reproduces the PDO pattern [Park et al., 2013], and we could also find the similarity between observational and simulated spatial features of the PDO from Fig. 1.

The SWM was used to examine the atmospheric wave response to different source regions. It is a fully nonlinear baroclinic model with a dry dynamical core and 14 vertical levels on sigma coordinates, and horizontal resolution is truncated at rhomboidal 30 (R30). The model experiment was designed to have an idealized forcing function corresponding to the transient vorticity, which has a sine-squared functional form (see Liu et al. [1998] and Schubert et al. [2011] for further details). The background state for the SWM is given by the full three-dimensional climatological flow from October to November reanalysis data.

3. Climatic impacts of the PDO and the warm Arctic during the late autumn

The PDO is known to exert various climatic impacts on NA and its adjacent regions during winter. Under the warm phase of the PDO, i.e., a warm anomaly along the western coast of NA and a cold anomaly in the central North Pacific, NA tends to experience anomalously warm (cold) temperatures over the northwest (the southeast) [*Mantua and Hare*, 2002; *Wang et al.*, 2013].

Associated with the PDO, the surface air temperature (SAT) exhibits a pronounced seasonal evolution as shown in Fig. 1. In October, the strong anomalous cold is dominant over the central NA region, then it weakens gradually and shifts eastward during the winter. These evolutionary features in the observation are reproduced well in the CM2.1 model (Fig. 1b), although the intensity of Z300 response is much weaker than the observation. The change in the SAT is

accompanied with an overlying atmospheric circulation, which is similar to the Pacific-North America (PNA) pattern, including an anomalously deep Aleutian low, an enhanced ridge over northwestern North America, and a downstream trough [*Wallace and Gutzler*, 1981]. This pattern is known as an amplified climatological stationary wave pattern, which eases southward advance of the arctic cold air masses that bring the cold anomaly to southeastern NA [*Leathers and Palecki*, 1991]. In fact, the cold anomaly is attributed to cold advection due to enhanced northerly winds (see Supplementary Fig. 1). Considering the stronger temperature response over NA in October and November seen in Fig. 1, we focus on the late autumn season in this study.

We examined the climatic impacts of arctic condition on the atmospheric circulation patterns corresponding to the PDO. In order to represent the arctic condition of the Pacific sector, we used the arctic temperature index (ART2 index) suggested by Kug et al. [2015], which is defined as the SAT averaged over the East Siberian-Chukchi Sea region (160°E–160°W, 65°N–80°N) (see Supplementary Fig. 2 for relevant circulation features with the ART2 index). When the PDO and the arctic condition are under warm and cold phases, respectively, (PDO > 0 and ART2 < 0), the temperature and the pressure anomalies in NA show a typical +PDO distribution, leading to northwestern warm and southeastern cold temperatures (Fig. 2a). On the other hand, there is quite a different situation when the arctic condition is warm (ART2 > 0). The ridge over northwestern NA moves westward so as to span the

offshore NA region and the subarctic coast, and the downstream trough moves farther inland (Fig. 2b). The altered pressure system enhances the cold anomaly in the central NA region. These altered characteristics of the PDO teleconnection by a warm Arctic are found consistently in the model output (Fig. 2d), although the magnitudes of the anomalies are smaller than those observed. The weaker cold anomaly over central NA in Fig. 2d is partly due to a weaker meridional temperature gradient in the climatology of model atmosphere (figure not shown).

4. Physical understanding of the modulation effect of a warm Arctic

In simple terms, the altered PDO teleconnection patterns by the Arctic may be regarded as a superposition of a conventional PDO teleconnection and a direct atmospheric response to a warm and a cold Arctic. According to Kug et al. [2015], the warm arctic surface condition over the East Siberian-Chukchi Sea often accompanies upper-level anticyclonic and downstream cyclonic anomalies over NA during the winter (December-February). In the late autumn, however, there is no pronounced downstream response over NA (Supplementary Fig. 2a). It is interesting that in spite of the smaller downstream impact of the warm Arctic during the late autumn, the downstream branch of the PDO response strengthens and results in a colder NA under the warm Arctic condition, as shown in Fig. 2. In order to clarify these nonlinear rectification impacts, we compared the PDO teleconnection patterns during the warm and the cold arctic years after removing the direct atmospheric

responses to the arctic surface conditions (Fig. 3). This was implemented by calculating linear regressions onto the PDO index for the subdivision of data according to the sign of the ART2 index. Since the linear regression uses deviations from the temporal average of a variable, the regression coefficients solely for cold (warm) arctic years indicate the PDO teleconnection pattern in which the general circulation features of the cold (the warm) arctic years are removed.

Interestingly, the ridge over northwestern NA and the downstream trough show noteworthy differences between Figs. 3a and 3b regarding the shape and the location. The ridge extends westward corresponding to the warm arctic condition, and the center of the downstream trough is shifted westward as well. In Fig. 3b, a steeper slope between the ridge and the downstream trough enables the stronger northerly winds to bring colder advection over central NA. In the observations, we see much colder surface air temperature anomalies prevailing over central NA. The model results also reproduce the similar characteristics of the atmospheric circulation (Figs. 3d and 3e). The only difference from the observations is that the magnitudes of the cold anomalies over NA are almost comparable between the warm and the cold arctic conditions in the model. However, the spatial distribution of cold anomalies seems consistent with that of the observations in which the cold anomaly dominates more over the central northern NA region under the warm arctic condition. The warm anomalies over Alaska show more pronounced differences between the cold and the warm arctic conditions and the observations and model

outputs are quite consistent. Figures 3c and 3f, the difference maps between the warm and the cold arctic conditions, show the distinct impacts of the PDO more clearly. These can be interpreted as nonlinear rectification impacts of the warm Arctic on the teleconnection pattern relevant to the +PDO. The consistency between the observations and the model supports that the warm arctic modulation on the midlatitude teleconnection pattern is not simply due to the linear combination of the direct atmospheric responses to arctic surface warming and the PDO. It is possibly due to the underlying nonlinear process.

The altered Rossby wave patterns in Fig. 3 might be attributed to different tropical Pacific origins. As the SAT anomalies given in Fig. 3 suggest, however, there is no noteworthy characteristic in the tropical Pacific. While an El Niño-like anomaly seems stronger in the warm arctic regression of the observations, it is not the same in the model output. Rather than suggesting a tropical source, the different responses to the arctic conditions may be related more to the atmospheric internal process in the extratropics. A large portion of the extratropical low-frequency variability is attributed to internal mechanisms such as barotropic instability and transient eddy forcing [*Hoskins and Karoly*, 1981; *Held*, 1983; *Luo et al*., 2016]. The transient vorticity flux in the storm track region is suggested to be crucial in driving a barotropic response in the atmosphere linked to the extratropical SST anomalies [*Ting and Peng*, 1995; *Peng and Whitaker*, 1999; *Li*, 2004; *Lim*, 2015].

Therefore, we examined the behaviors of the Pacific storm track in order to

understand the physical link between the altered wave responses to the PDO and the arctic condition. Storm track activity over the North Pacific was defined as follows. 2-8 day band-pass filter was applied to meridional wind at 300 hPa so as to leave the transient component only, and its variance was then defined as the storm track activity. It is known that oceanic anomalies corresponding to the PDO change the meridional temperature gradient in the planetary boundary layer (PBL) across the Pacific and affect the anchorage of the storm track over the North Pacific [*Bond and Harrison*, 2000; *Sung et al.*, 2014]. In Figs. 4a and 4c, we can see such modulation of the storm track activity with respect to the PDO under the cold arctic conditions for the observations and the CM2.1 output, respectively. Compared to the climatological distribution of the North Pacific storm track (shading), the anomalies relevant to +PDO tend to shift equatorward being centered over 160°W, 40°N (contour). Conspicuously, the shift of the storm track accompanied by the +PDO seems farther equatorward when the arctic surface is under warm conditions (Figs. 4b and 4d), although the shift is not as large in the model as in the observation. The weaker response in the model is possibly due to weaker air-sea interaction in the model [Kushnir et al., 2002]. The consistent shift of the storm track farther equatorward under the warm arctic conditions in the observations and the model may imply that the warm Arctic modulates the atmospheric baroclinicity so that the PDO-related SST anomaly can lead to greater shift of the storm track.

In fact, it is not new that warming at the surface of the polar region is

associated with an equatorward shift of the storm track [*Butler et al.*, 2010; *Inoue et al., 2012*]. Moreover, a recent study by Yim et al. [2015] shows convincing evidence to support the impact of the warm Arctic on the atmospheric baroclinicity, which can be assessed by the meridional movement of the midlatitude jet stream. In the Coupled Model Intercomparison Project Phase 5 (CMIP5) simulations, they found large inter-model diversity in the behaviors of the midlatitude jet under greenhouse warming. By extension, it is also identified that inter-model differences are highly dependent on the intensity of the arctic surface warming simulated in each model, i.e., the midlatitude jet tends to shift equatorward in the models with a stronger arctic surface warming tendency.

The impact of the altered storm track on the large-scale circulation was tested using the SWM experiments by prescribing transient vorticity forcing corresponding to the different arctic conditions. Figure 4e shows responses to idealized vorticity sources given in two selected locations where anomalous storm activities dominate, i.e., 160°W, 40°N (P1) and 160°W, 30°N (P2), as shown in Figs. 4a and 4b, respectively. Interestingly, the response to the transient vorticity forcing located at P1 (shading) resembles the circulation anomalies shown in Figs. 3a and 3d, which correspond to the +PDO under the cold arctic condition, while the response to the vorticity source at P2 is similar to those in Figs. 3b and 3e, which display westward shifted circulation anomalies under the warm arctic condition. The agreement between the SWM responses to the anomalous vorticity forcing and the observed circulation

anomalies implies that the transient vorticity forcing due to the altered storm track can be critical in generating different Rossby wave train patterns. This is in good agreement with Lim [2015] and Franzke and Feldstein [2005], which showed that an anomalous vorticity transient near the midlatitude storm track can be more important than the diabatic heating for generating certain atmospheric teleconnection patterns. These results also lend credence to the arguments that the warm Arctic can lead to anomalous cold over central NA by modulating the atmospheric teleconnection.

5. Discussion

In the literature, controversial arguments exist about the origin of the recurring cold winters in North America, as mentioned in the introduction. Researchers who emphasize the role of a warm Arctic present the reasons as the weakened meridional difference in thickness, which leads to weaker thermal winds, and the consequential amplification of the midlatitude atmospheric planetary waves [*Overland and Wang*, 2010; *Francis and Vavrus*, 2015]. However, it is still debated whether the warm Arctic really causes a wavier Northern Hemispheric circulation [*Barnes*, 2013; *Screen et al*., 2013; *Wallace et al*., 2014]. Our results suggest the influence of the reduced meridional thickness gradient on the low-frequency atmospheric wave in association with the transient vorticity forcing. Although the focus of the current study was the late autumn season, the physical process relevant to the

atmospheric baroclinicity and the transient vorticity flux could be applied for the growth of low-frequency waves in the winter as well.

Recently, Lee et al. [2015] have shown model experiments for one of the most severe winters, i.e., the winter of 2013/14 in NA (See Fig. 5a which shows distinct cold anomalies over central NA). Through numerical simulations with various lower boundary forcings, they suggested that the anomalous SST in the North Pacific and the reduced sea ice during the 2013/14 winter could intensify internal variabilities, such as North Pacific Oscillation pattern (NPO), so as to bring the exceptional cold winter over the NA region. Their point is quite consistent with ours, which ascribes the origin of the cold weather to the North Pacific SST and the warm Arctic, although the underlying process was not noted in their work. In the present study, by extension, a general relationship was addressed in addition to the physical mechanism for bringing cold weather to NA from the perspective of the PDO. It is supposed that the behaviors of the storm track could be also pertinent to the strengthened NPO variability during the 2013/14 winter, as a synthesis of the results from the anomalous SST structure and the arctic condition At that time, actually, anomalous storm track activity was observed over the eastern North Pacific where the abnormal warming of the SST is pronounced (Figs. 5b). The corresponding SWM response to the transient vorticity forcing at 160°W, 35°N shows consistent features with the observed Z300 anomalies (Figs. 5a and 5c), possibly implying that the amplified NPO variability is due to the anomalous transient vorticity.Note that the

arctic was abnormally warm for the period. Nevertheless, it is still uncertain whether the warm arctic really exerted modulation effect to the anomalous storm track activity. We plan to explore this in the following study, focusing on the winter season NA cold.

According to Lu et al. [2007], an increase in the subtropical static stability, which causes the expansion of the Hadley cell, acts to push the baroclinic instability zone poleward. As suggested previously, the baroclinic instability zone is also responsive to the surface boundary conditions, such as the PDO [*Bond and Harrison*, 2000; *Sung et al.*, 2014]. Although observations and model experiments show consistent results, the mechanism by which the local surface warming in the narrow arctic region changes the midlatitude atmospheric baroclinicity over the vast expanse of the North Pacific remains unclear. Understanding the potential impact of the Arctic on the internal midlatitude processes is a complicated but important problem, since this may hold the key to understanding, not only the cold winter, but also a recent severe drought in California, which is in the downstream zone of the Pacific storm track [*Griffin and Anchukaitis*, 2014]. This motivates further study on the interaction between the arctic and the subarctic circulations.

Acknowledgements

NCEP Reanalysis data used for this paper are provided by the NOAA/OAR/ESRL PSD, Boulder, Colorado, USA, from their Web site at http://www.esrl.noaa.gov/psd/. Monthly SST data are downloaded from http://www.metoffice.gov.uk/hadobs/hadisst/. This study was supported by

KMIPA2015-2093 (PN15040) of the Korean government and "Development and Application of the Korea Polar Prediction System (KPOPS) for Climate Change and Weather Disaster (PE16100)" project.

References

Barnes, E. A. (2013), Revisiting the evidence linking Arctic amplification to extreme weather in midlatitudes, *Geophysical Research Letters*, *40*(17), 4734-4739.

Bond, N. A., and D. Harrison (2000), The Pacific decadal oscillation, air-sea interaction and central north Pacific winter atmospheric regimes, *Geophysical Research Letters*, *27*(5), 731-734.

Butler, A. H., D. W. Thompson, and R. Heikes (2010), The steady-state atmospheric circulation response to climate change-like thermal forcings in a simple general circulation model, *Journal of Climate*, *23*(13), 3474-3496.

Delworth, T. L., et al., (2006), GFDL's CM2 global coupled climate models. Part I: formation and simulation characteristics, *J. Clim.*, *19*, 634-674.

Francis, J. A., and S. J. Vavrus (2015), Evidence for a wavier jet stream in response to rapid Arctic warming, *Environmental Research Letters*, *10*(1), 014005.

Frankignoul, C., N. Sennéchael, Y.-O. Kwon, and M. A. Alexander (2011), Influence of the Meridional Shifts of the Kuroshio and the Oyashio Extensions on the Atmospheric Circulation, *J. Clim.*, *24*(3), 762-777.

Franzke, C., and S. B. Feldstein (2005), The continuum and dynamics of Northern Hemisphere teleconnection patterns, *Journal of the atmospheric sciences*, *62*(9), 3250-3267.

Griffin, D., and K. J. Anchukaitis (2014), How unusual is the 2012–2014 California drought?, *Geophysical Research Letters*, *41*(24), 9017-9023.

Hartmann, D. L. (2015), Pacific sea surface temperature and the winter of 2014, *Geophysical Research Letters*, *42*(6), 1894-1902.

Held, I. M. (1983), *Stationary and quasi-stationary eddies in the extratropical troposphere: Theory. Large-Scale Dynamical Processes in the Atmosphere*, Academic Press.

Hoskins, B. J., and D. J. Karoly (1981), The Steady Linear Response of a Spherical Atmosphere to Thermal and Orographic Forcing, *J. Atmos. Sci.*, *38*, 1179-1196.

Inoue, J., M. E. Hori, and K. Takaya (2012), The role of Barents sea ice in the wintertime cyclone track and emergence of a warm-Arctic cold-Siberian anomaly. *J. Climate*, 25, 2561-2568.

Kug, J. S., and F. F. Jin (2009), Left-hand rule for synoptic eddy feedback on low-frequency flow, *Geophys. Res. Lett*, *36*, L05709.

Kug, J. S., J.-H. Jeong, Y.-S. Jang, B.-M. Kim, C. K. Folland, S.-K. Min, and S.-W. Son (2015), Two distinct influences of Arctic warming on cold winters over North America and East Asia, *Nature Geoscience*, *8*, 759-762.

Kushnir, Y., W. A. Robinson, I. Blade, N. M. J. Hall, S. Peng, and R. Sutton (2002), Atmospheric GCM response to extratropical SST anomalies: synthesis and evaluation*, *J. Clim.*, *15*(16), 2233-2256.

Lau, N. C., and M. J. Nath (1994), A modeling study of the relative roles of tropical and extratropical SST anomalies in the variability of the global atmosphere-ocean system, *J. Clim.*, *7*, 1184-1207.

Leathers, D. J., and M. A. Palecki (1991), The Pacific/North American teleconnection pattern and United States climate. Part I: REgional Temperature and Precipitation Associations, *J. Clim.*, *4*, 517-528.

Lee, M.-Y., C.-C. Hong, and H.-H. Hsu (2015), Compounding effects of warm sea surface temperature and reduced sea ice on the extreme circulation over the extratropical North Pacific and North

America during the 2013-2014 boreal winter, *Geo. Res. Lett.*, *42*, 1612-1618.
Li, S. (2004), Impact of Northwest Atlantic SST anomalies on the circulation over the Ural Mountains during early winter, *J. Meteor. Soc, Japan*, *82*(4), 971-988.
Lim, Y.-K. (2015), The East Atlantic/West Russia (EA/WR) teleconnection in the North Atlantic: climate impact and relation to Rossby wave propagation, *Climate Dynamics*, *44*(11-12), 3211-3222.
Liu, A. Z., M. Ting, and H. Wang (1998), Maintenance of circulation anomalies during the 1988 drought and 1993 floods over the United States, *Journal of the atmospheric sciences*, *55*(17), 2810-2832.
Lu, J., G. A. Vecchi, and T. Reichler (2007), Expansion of the Hadley cell under global warming, *Geophysical Research Letters*, *34*(6).
Luo, D., Y. Xiao, Y. Diao, A. Dai, C. L. E. Franzke, I. Simmonds (2016), Impacts of Ural Blocking on Winter Warm Arctic-Cold Eurasian Anomalies. Part II: The Link to the North Atlantic Oscillation, *J. Clim.*, *29*(11), 3949-3971.
Mantua, N. J., and S. R. Hare (2002), The Pacific decadal oscillation, *Journal of Oceanography*, *58*(1), 35-44.
Overland, J. E., and M. Wang (2010), Large scale atmospheric circulation changes are associated with the recent loss of Arctic sea ice, *Tellus A*, *62*(1), 1-9.
Overland, J. E., and M. Wang (2015), Increased Variability in the Early Winter Subarctic North American Atmospheric Circulation*, *Journal of Climate*, *28*(18), 7297-7305.
Palmer, T. (2014), Record-breaking winters and global climate change, *Science*, *344*(6186), 803-804.
Park, J.-H., S.-I. An, S.-W. Yeh, and N. Schneider (2013), Quantitative assessment of the climate components driving the pacific decadal oscillation in climate models, *Theor. Appl. Climatol.*, 1-15.
Peng, S., and J. S. Whitaker (1999), Mechanisms determining the atmospheric response to midlatitude SST anomalies, *Journal of Climate*, *12*(5), 1393-1408.
Sampe, T., H. Nakamura, A. Goto, and W. Ohfuchi (2010), Significance of a Midlatitude SST Frontal Zone in the Formation of a Storm Track and an Eddy-Driven Westerly Jet*, *J. Clim.*, *23*(7), 1793-1814.
Sato K, Inoue J and Watanabe M (2014), Influence of the Gulf Stream on the Barents Sea ice retreat and Eurasian coldness during early winter, *Environ. Res. Lett. 9,* 084009
Schneider, N., and B. D. Cornuelle (2005), The Forcing of the Pacific Decadal Oscillation*, *J. Clim.*, *18*(21), 4355-4373.
Schubert, S., H. Wang, and M. Suarez (2011), Warm season subseasonal variability and climate extremes in the Northern Hemisphere: The role of stationary Rossby waves, *Journal of Climate*, *24*(18), 4773-4792.
Screen, J. A., and I. Simmonds (2010), Increasing fall-winter energy loss from the Arctic Ocean and its role in Arctic temperature amplification, *Geophys. Res. Lett.*, *37*(16), L16707.
Screen, J. A., I. Simmonds, C. Deser, and R. Tomas (2013), The Atmospheric Response to Three Decades of Observed Arctic Sea Ice Loss, *J. Clim.*, *26*, 1230-1248
Simmonds, I., and P. D. Govekar (2014), What are the physical links between Arctic sea ice loss and Eurasian winter climate, *Environ. Res. Lett.*, *9*, 101003
Smith, T. M., R. W. Reynolds, T. C. Peterson, and J. Lawrimore (2008), Improvements NOAAs Historical Merged Land–Ocean Temp Analysis (1880–2006), *Journal of Climate*, *21*, 2283-2296.
Stroeve, J. C., V. Kattsov, A. Barrett, M. Serreze, T. Pavlova, M. Holland, W. N. Meier (2012), Trends in Arctic sea ice extent from CMIP5, CMIP3 and observations, *Geophysical Research Letters, 39*(16), L16502
Sung, M. K., S. I. An, B. M. Kim, and S. H. Woo (2014), A physical mechanism of the precipitation dipole in the western United States based on PDO-storm track relationship, *Geophysical Research Letters*, *41*(13), 4719-4726.
Ting, M., and S. Peng (1995), Dynamics of the early and middle winter atmospheric responses to the northwest Atlantic SST anomalies, *Journal of climate*, *8*(9), 2239-2254.

Ting, M., and L. Yu (1998), Steady response to tropical heating in wavy linear and nonlinear baroclinic models, *Journal of the atmospheric sciences*, *55*(24), 3565-3582.

Wallace, J. M., and D. S. Gutzler (1981), Teleconnections in the Geopotential Height Field during the Northern Hemisphere Winter, *Mon. Wea. Rev.*, *109*, 784-812.

Wallace, J. M., I. M. Held, D. W. J. Thompson, K. E. Trenberth, and J. E. Walsh (2014), Global warming and winter weather, *Science*, *343*, 729-730.

Wang, F., Z. Liu, and M. Notaro (2013), Extracting the dominant SST modes impacting North America's observed climate*, *Journal of Climate*, *26*(15), 5434-5452.

Yim, B. Y., H. S. Min, and J.-S. Kug (2015), Inter-model diversity in jet stream changes and its relation to Arctic climate in CMIP5, *Climate Dynamics*, 1-14.

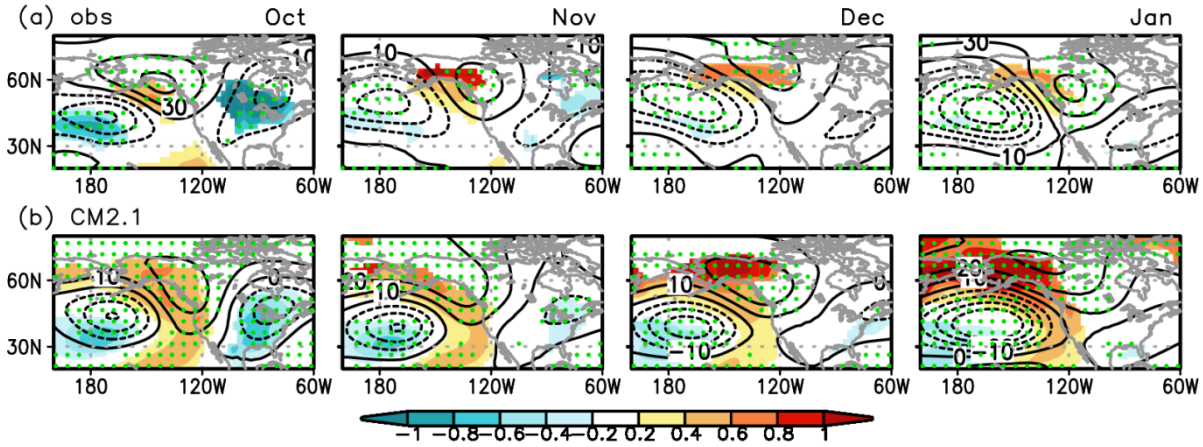

Figure 1. Monthly surface air temperature (shading) and geopotential height at 300 hPa (contour) anomalies regressed onto the PDO index from October to January in (a) observation and (b) CM2.1 output. Contour intervals are 20 m (10 m) for the observation (the model), and the temperature anomalies, which are significant at a 95% confidence level, were shaded only. Stippled areas indicate a significant deviation of Z300 at 99% confidence level.

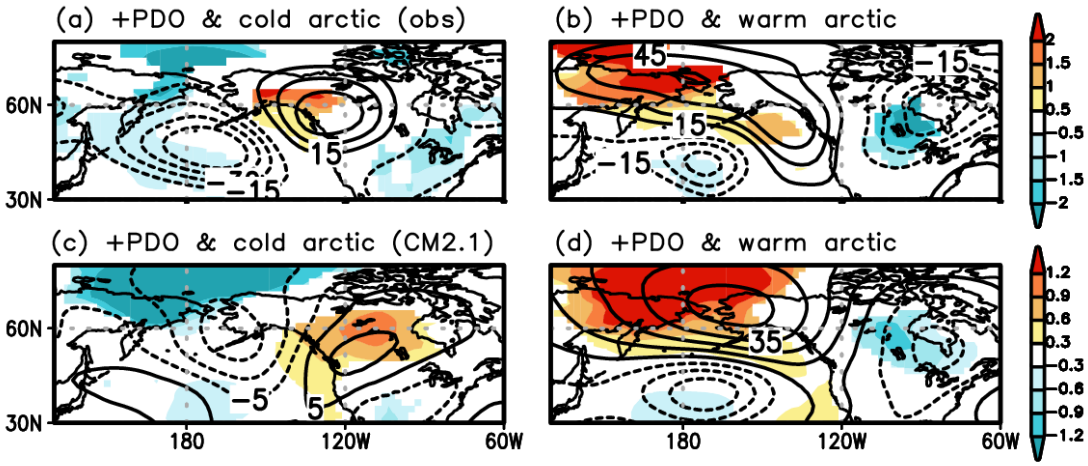

Figure 2. Observed Z300 (contour) and SAT (shading) anomalies during +PDO years accompanied by (a) cold (15 years) and (b) warm (8 years) arctic conditions, respectively. (c)-(d) Same as (a)-(b) except for CM2.1 model output, which considers 64 (79) cold (warm) arctic years. Contour intervals are 15 m (10 m) for the observation (the model), and the temperature anomalies, which are significant at a 95% confidence level, were shaded only. Note that the scales are different between observation and model.

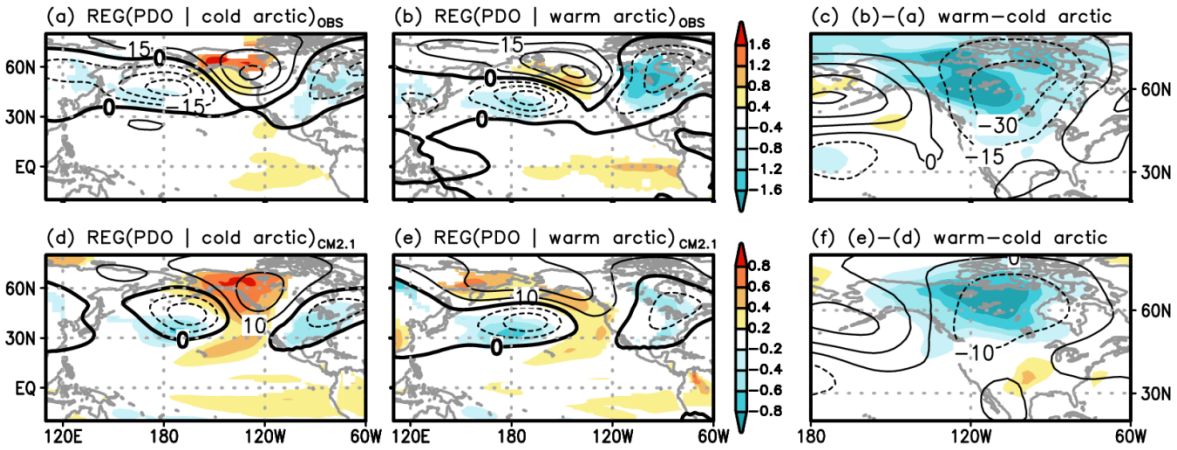

Figure 3. Observed Z300 (contour) and SAT (shading) anomalies regressed onto PDO index for (a) cold arctic (40 years) and (b) warm arctic (22 years) years, respectively. Temperature anomalies, which are significant at a 95% confidence level, were shaded only. (c) Difference between (a) and (b). (d)-(f) are same as (a)-(c) except for the CM2.1 output with 149 cold and 151 warm arctic years. The thick black contour denotes the zero line, and contour intervals are 15 m (10 m) for the observations (the model). Note that the scales are different between observation and model.

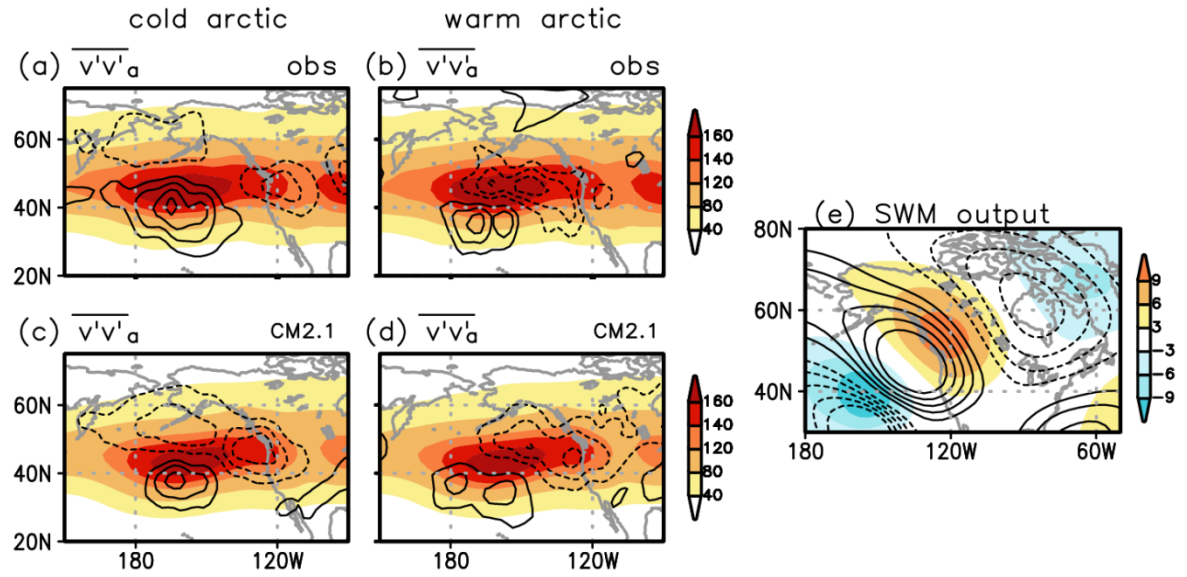

Figure 4. Storm track activity (contour) regressed onto the PDO index for (a) cold and (b) warm arctic years for the observations. Shading denotes climatological storm track activity. (c) and (d) are same as (a)-(b), but for the CM2.1 output. Contour intervals are 6 m^2s^{-2} (3 m^2s^{-2}) for the observations (the model), and the zero line is omitted. (e) Average streamfunction response integrated for ~30 days (divided by 10^5) of the stationary wave model to the transient vorticity forcing located over 160°W, 40°N (shading) and 160°W, 30°N (contour).

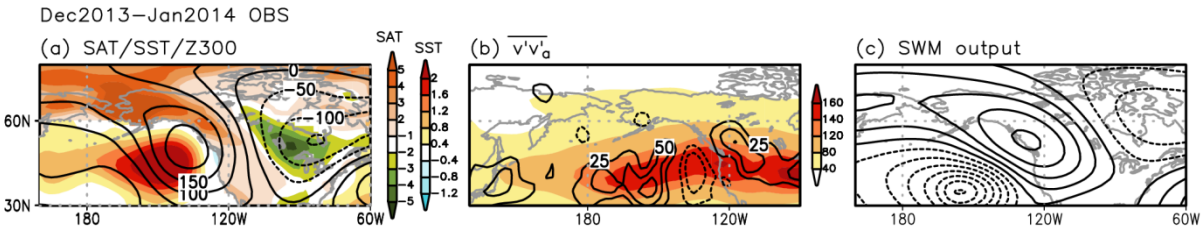

Figure 5. (a) Observed SAT, SST (shading), and Z300 anomalies (contour) for 2013/14 winter (December to January), and (b) corresponding storm track activity anomaly (contour). Shading denotes climatology. (c) Average streamfunction response integrated for ~30 days (divided by 10^5) of the stationary wave model to the transient vorticity forcing located over 160°W, 35°N. Contour interval is $2m^2s$.

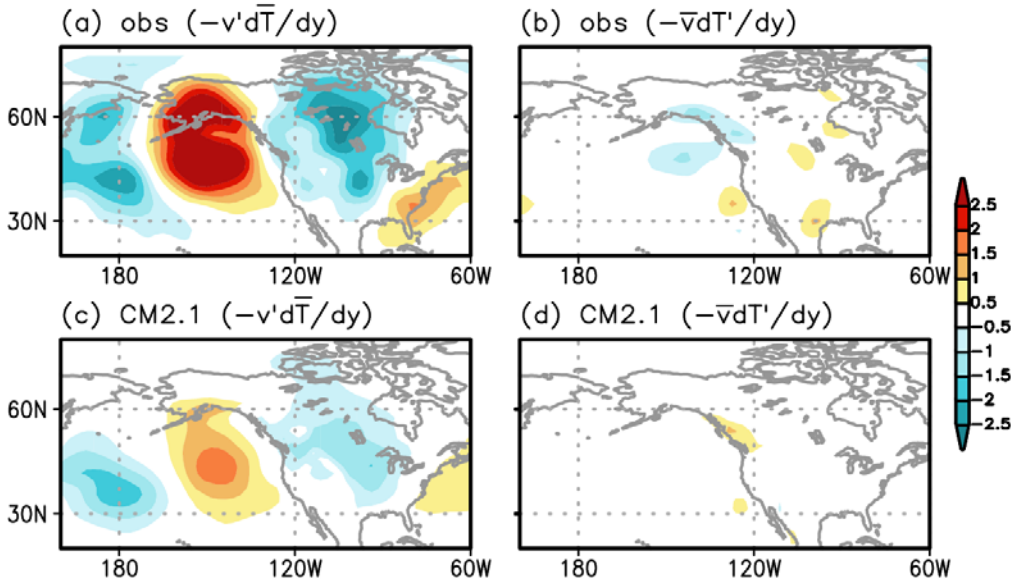

Supplementary Figure 1. Contributions by meridional advection at 850 hPa in the temperature anomalies associated with the PDO during October to November. The overbar and prime denote the monthly climatology and its deviation, respectively.

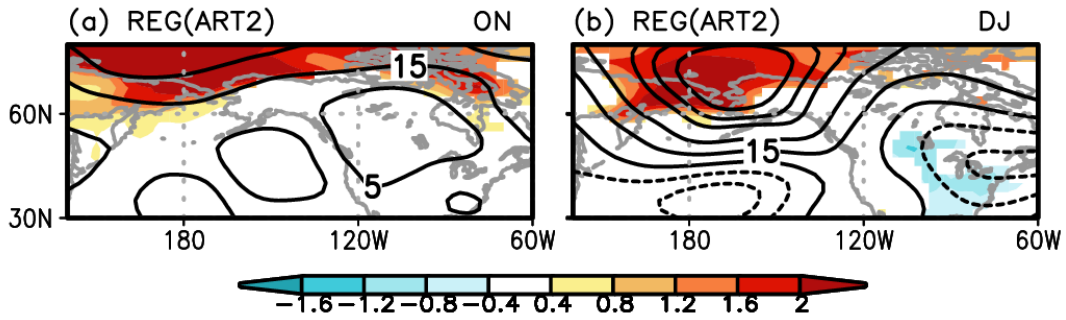

Supplementary Figure 2. The observed surface air temperature (shading) and the geopotential height at 300 hPa (contour) anomalies regressed onto the ART2 index during (a) October to November and (b) December to January. The contour intervals are 10 m, and the temperature anomalies significant at a 95% confidence level were shaded only.